nature cell biology

The tumour suppressor RASSF1A regulates mitosis by inhibiting the APC–Cdc20 complex

Min Sup Song[1,2], Su Jeong Song[1], Nagi G. Ayad[3], Jin Sook Chang[1], Joo Hyun Lee[1], Hyun Kyung Hong[1], Ho Lee[1], Naeyun Choi[4], Jhingook Kim[4], Hojoong Kim[4], Jin Woo Kim[2], Eui-Ju Choi[2], Marc W. Kirschner[3] and Dae-Sik Lim[1]

The tumour suppressor gene *RASSF1A* is frequently silenced in lung cancer and other sporadic tumours as a result of hypermethylation of a CpG island in its promoter[1–6]. However, the precise mechanism by which RASSF1A functions in cell cycle regulation and tumour suppression has remained unknown. Here we show that RASSF1A regulates the stability of mitotic cyclins and the timing of mitotic progression. RASSF1A localizes to microtubules during interphase and to centrosomes and the spindle during mitosis. The overexpression of RASSF1A induced stabilization of mitotic cyclins and mitotic arrest at prometaphase. RASSF1A interacts with Cdc20, an activator of the anaphase-promoting complex (APC), resulting in the inhibition of APC activity. Although RASSF1A does not contribute to either the Mad2-dependent spindle assembly checkpoint or the function of Emi1 (ref. 1), depletion of RASSF1A by RNA interference accelerated the mitotic cyclin degradation and mitotic progression as a result of premature APC activation. It also caused a cell division defect characterized by centrosome abnormalities and multipolar spindles. These findings implicate RASSF1A in the regulation of both APC–Cdc20 activity and mitotic progression.

Mitotic progression requires the degradation of mitotic regulatory proteins. The anaphase-promoting complex (APC), a ubiquitin ligase, specifically targets mitotic cyclins A and B to allow mitotic progression[7–10]. Two proteins, Cdc20 and Cdh1, bind directly to the APC and thereby activate APC in mitosis and in G1 phase, respectively[11]. Mad2 and the spindle assembly checkpoint pathway inhibit APC–Cdc20 in response to spindle damage, and the early mitotic inhibitor Emi1 inhibits both Cdc20 and Cdh1 in S and G2 phases[12–14]. However, additional APC regulators probably exist to ensure the destruction of APC substrates at the right time and place.

Two major isoforms of RASSF1, A and C, are produced from the human *RASSF1* gene on chromosome 3p21.3 (ref. 1). RASSF1A contains a cysteine-rich diacylglycerol-binding domain (C1 domain) in its amino-terminal region and a Ras-association (RA) domain. RASSF1C contains the RA domain but the C1 domain is replaced in this protein by a distinct 50-amino-acid sequence[1,3]. RASSF1C is thought to play a role in RAS-mediated cellular activities[15], whereas RASSF1A is implicated in cell cycle progression at the G1–S transitition[16]. The inhibition of cell growth by ectopic expression of RASSF1A, but not by RASSF1C, is indicative of a tumour suppressor function of RASSF1A[1,16].

To investigate the function of RASSF1A in cell division, we first examined the subcellular localization of this protein by immunofluorescence analysis. A substantial proportion of haemagglutinin epitope (HA)–tagged RASSF1A seemed to be localized to an array of microtubules that coursed from the perinuclear region to the periphery of HeLa cells (Fig. 1a). In contrast, most HA–RASSF1C staining was localized to the nucleus with a diffuse or punctate distribution. Treatment of cells with colchicine, a microtubule-disrupting agent, disturbed both the organization of microtubules and the pattern of HA–RASSF1A staining (Fig. 1a), supporting the localization of RASSF1A to microtubules.

We next generated polyclonal antibodies either against a carboxy-terminal peptide of human RASSF1 or against full-length RASSF1A (anti-RASSF1(331) or anti-RASSF1(A4), respectively). These antibodies specifically recognized both the endogenous protein and Flag-epitope-tagged RASSF1A expressed in HeLa cells with the expected molecular mass of about 44 kDa (Fig. 1b). The specificity of the antibodies was confirmed by the observation that they did not detect RASSF1A in RASSF1A-deficient lung cancer cell lines, whereas they did detect this protein in the same cell lines after exposure of the cells to 5-aza-2′-deoxycytidine, an inhibitor of DNA methylation (Fig. 1b). Endogenous RASSF1A was also localized to cytoplasmic microtubules during interphase (Fig. 1b) and to bipolar centrosomes associated with microtubules during prophase, to spindle fibres and spindle poles at metaphase and anaphase, to the midzone during early telophase, and to the midbody in late telophase (Fig. 1c) in cells.

Next we examined the effect of RASSF1A overexpression on the cell cycle after transient co-transfection with vectors for RASSF1A and

[1]Department of Biological Sciences, Korea Advanced Institute of Science and Technology, 373-1 Guseoung-D, Yuseong-G, Daejeon 305-701, Korea. [2]School of Life Science and Biotechnology, Korea University, 1,5-Ka Anam-Dong, Sungbuk-G, Seoul 136-701, Korea. [3]Department of Cell Biology, Harvard Medical School, 2000 Longwood Avenue, Boston, MA 02115, USA. [4]Samsung Medical Center, 50-Ka Ilweon-D, Kangnam-G, Seoul 135-230, Korea. Correspondence should be addressed to D.S.L. (daesiklim@kaist.ac.kr).

Published online: 25 January 2004; DOI: 10.1038/ncb1091

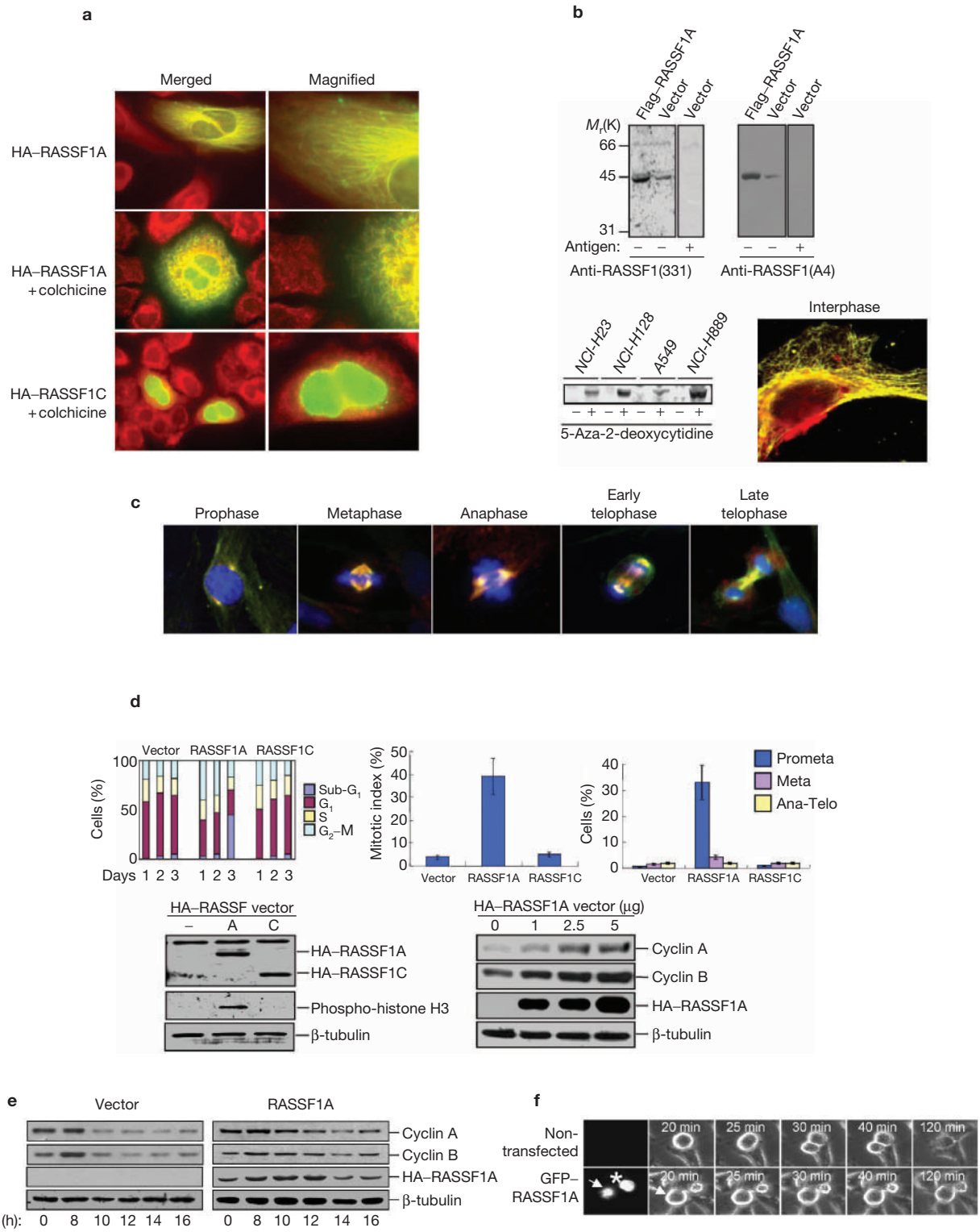

CD4 (surface marker). Flow cytometric analysis revealed that overexpression of RASSF1A induced G2–M arrest, whereas RASSF1C had no effect on cell cycle distribution (Fig. 1d). Furthermore, RASSF1A markedly increased the mitotic index, and most of the RASSF1A-overexpressing cells were in prometaphase (Fig. 1d). RASSF1A induced the phosphorylation of histone H3 in HeLa cells and increased the abundance of cyclins A and B in 293T cells in a dose-dependent manner (Fig. 1d), which is consistent with cell cycle arrest at prometaphase.

We then determined the duration of the mitotic arrest induced by RASSF1A overexpression in HeLa cells synchronized by the double thymidine block protocol. Whereas most control cells had progressed from prometaphase to anaphase–telophase by 11 h after release from the thymidine block, the proportion of RASSF1A-overexpressing cells in prometaphase remained above 80% at this time (data not shown).

Figure 1 RASFF1A localizes to microtubules and induces mitotic arrest at prometaphase. (**a**) HeLa cells were transiently transfected with plasmids encoding HA-tagged RASSF1-A or RASSF1-C, cultured for 30 min in the absence or presence of colchicine (1 mg ml^{-1}), fixed and stained. Yellow staining in the merged images indicates co-localization of HA–RASSF1A (green) and β-tubulin (red). (**b**) Characterization of anti-RASSF1. Lysates of HeLa cells transiently transfected with a vector for Flag–RASSF1A or the corresponding empty vector were subjected to immunoblot analysis with anti-RASSF1(331) or anti-RASSF1(A4). The antibodies were pretreated with antigen as a control in the right lanes. RASSF1A-deficient cell lines were also incubated for 72 h in the absence or presence of 5-aza-2′-deoxycytidine (2 μM), lysed, and analysed with anti-RASSF1(331). Interphasic HeLa cells were stained with this antibody. (**c**) Mitotic HeLa cells were stained with anti-RASSF1A(331) (red), anti-α-tubulin (green) and DAPI (blue). (**d**) RASFF1A induces mitotic arrest at prometaphase accompanied by the accumulation of cyclins A and B. The DNA content of CD4-positive cells was determined by flow cytometry at the indicated days after transfection (left). The mitotic index of control or HA-positive cells and also the percentages of these cells in each mitotic phase were determined (middle and right). Data are means ± s.e.m. from three independent experiments. RASSF1A induced the phosphorylation of histone H3 and increased the abundance of cyclins A and B (bottom). (**e**) 293T cells transfected with an HA–RASSF1A vector or the empty vector were released from thymidine block for the indicated times, after which cell lysates were subjected to immunoblotting for the indicated proteins. (**f**) HeLa cells were transfected with a vector for GFP–RASSF1A and then examined by time-lapse microscopy every 5 min. The leftmost panels are fluorescence images; the remaining panels are phase-contrast images. Arrows indicate mitotic cells; asterisks indicate apoptotic cells expressing maximal levels of GFP–RASSF1A.

Consistently, the amounts of cyclins A and B in control cells were greatly reduced 10 h after release, whereas the accumulation of cyclins A and B apparent in RASSF1A-overexpressing cells was maintained for more than 14 h after release (Fig. 1e). Time-lapse microscopy also revealed that progression from prometaphase to telophase was complete within 30–40 min in control cells ($n = 6$), whereas cells expressing a green fluorescent protein (GFP)–RASSF1A fusion construct failed to progress from prometaphase to metaphase within 120 min ($n = 6$); those with high levels of GFP–RASSF1A expression underwent cell death ($n = 2$) (Fig. 1f). Thus, overexpression of RASSF1A, but not that of RASSF1C, inhibits cell growth by inducing mitotic arrest at prometaphase, and this arrest is accompanied by the accumulation of cyclins A and B.

The effects of RASSF1A overexpression, including early mitotic arrest and accumulation of mitotic cyclins, are similar to those previously described for the overexpression of Mad2 or Emi1, which negatively regulate APC–Cdc20 activity through association with Cdc20 (refs 12, 17). We therefore determined whether RASSF1A also binds to Cdc20 and thereby inactivates the APC–Cdc20 complex to allow the stabilization and accumulation of cyclins A and B. HA–Cdc20 was precipitated with Flag–RASSF1A from lysates of unsynchronized 293T cells, and endogenous RASSF1A was precipitated (although to a lesser extent) with endogenous Cdc20 from lysates of unsynchronized HeLa cells (Fig. 2a). A substantial proportion of endogenous RASSF1A was localized with endogenous Cdc20 to spindle poles and spindle fibres in HeLa cells at prometaphase (Fig. 2b). The amount of endogenous RASSF1A that precipitated with Cdc20 was maximal at prometaphase (Fig. 2b). These results were thus indicative of a physical interaction between RASSF1A and Cdc20 at prometaphase. Furthermore, we found that the N-terminal region of RASSF1A (RASSF1A-N, residues 1–109), but not the C-terminal region (RASSF1A-C, residues 110–340, containing the RA domain), interacted directly with the N-terminal region of Cdc20 (residues 1–100) *in vivo* and *in vitro* (Fig. 2c, d, and data not shown).

We then examined whether RASSF1A also inhibits APC activity as a result of its association with Cdc20. The ubiquitin ligase activity of APC derived from mitotic HeLa cells, activated by incubation with Cdc20 translated *in vitro*, was greatly inhibited by the full-length RASSF1A translated *in vitro* but not by the deletion mutant RASSF1A-C (Fig. 3a). Unexpectedly, RASSF1A-N also failed to inhibit APC activity, even though this mutant was able to bind to Cdc20, indicating that the inhibition of APC–Cdc20 by RASSF1A might involve more than simple binding. We then examined the effect of RASSF1A on APC–Cdc20 activity *in vivo* by measuring the extent of cyclin B ubiquitination during mitosis in cells expressing Flag–RASSF1A and HA–ubiquitin. At prometaphase, RASSF1A was sufficient to inhibit cyclin B ubiquitination (Fig. 3b). As expected, RASSF1A-N and RASSF1A-C failed to inhibit cyclin B ubiquitination and to induce the accumulation of mitotic cyclins and also to increase the mitotic index and to induce prometaphase arrest in cells (Fig. 3c). They also did not localize to interphase microtubules and to the mitotic spindle (data not shown), indicating that RASSF1A might prevent Cdc20 from activating the APC through its interaction with Cdc20 at the spindle apparatus *in vivo*. Furthermore, in cells released from thymidine block, ectopic expression of an excess of Cdc20 was able to overcome the delay in the destruction of mitotic cyclins induced by RASSF1A (Fig. 3d). These data thus indicate that the balance between RASSF1A and Cdc20 might be a determinant of APC activity and the subsequent destruction of mitotic cyclins.

Given that Mad2 and Emi1 are potent negative regulators of Cdc20 during mitotic progression[12,18], we examined whether RASSF1A contributes to such Mad2- and Emi1-dependent Cdc20 control during mitosis. We first restored RASSF1A expression in RASSF1A-deficient A549 lung cancer cells with a retroviral vector for this protein (Fig. 4a). We also used plasmid-based RNA interference (RNAi)[19] to deplete HeLa cells of endogenous RASSF1A; two out of three RASSF1A small interfering RNAs (siRNAs) stably suppressed RASSF1A expression in these cells (Fig. 4a). All of these modified A549 and HeLa cells underwent normal mitotic arrest in response to nocodazole-induced spindle damage (Fig. 4a), indicating that RASSF1A might not contribute to spindle assembly checkpoint control. It is of interest that overexpression of RASSF1A suppressed the spindle checkpoint defect induced by inactivation of Mad2 with RNAi or by overexpression of an N-terminal fragment of Cdc20 (refs 18, 20, 21). RASSF1A overexpression also inhibited the decrease in the level of cyclin B apparent after spindle damage in cells deficient in Mad2 function (Fig. 4b). In addition, RASSF1A overexpression induced both mitotic arrest and accumulation of cyclins A and B in cells depleted of Emi1 by RNAi in a manner similar to that apparent in control cells (Fig. 4c). We then determined the kinetics of the association of Cdc20 with Emi1, Mad2 and RASSF1A *in vivo* during mitotic progression. The association of Emi1 with Cdc20 occurred 4 h after release from thymidine block (prophase). In contrast, the association of RASSF1A or Mad2 with Cdc20 was evident between 8 and 12 h after release (prometaphase to metaphase), at the time of Emi1 destruction (Fig. 4d). Furthermore, neither Emi1 nor Mad2 was detected in RASSF1A immunoprecipitates prepared from A549 cells stably expressing HA–RASSF1A during mitotic progression (Fig. 4d). Taken together, these results indicate that RASSF1A-mediated regulation of Cdc20 might be independent of Mad2 and Emi1 during mitosis.

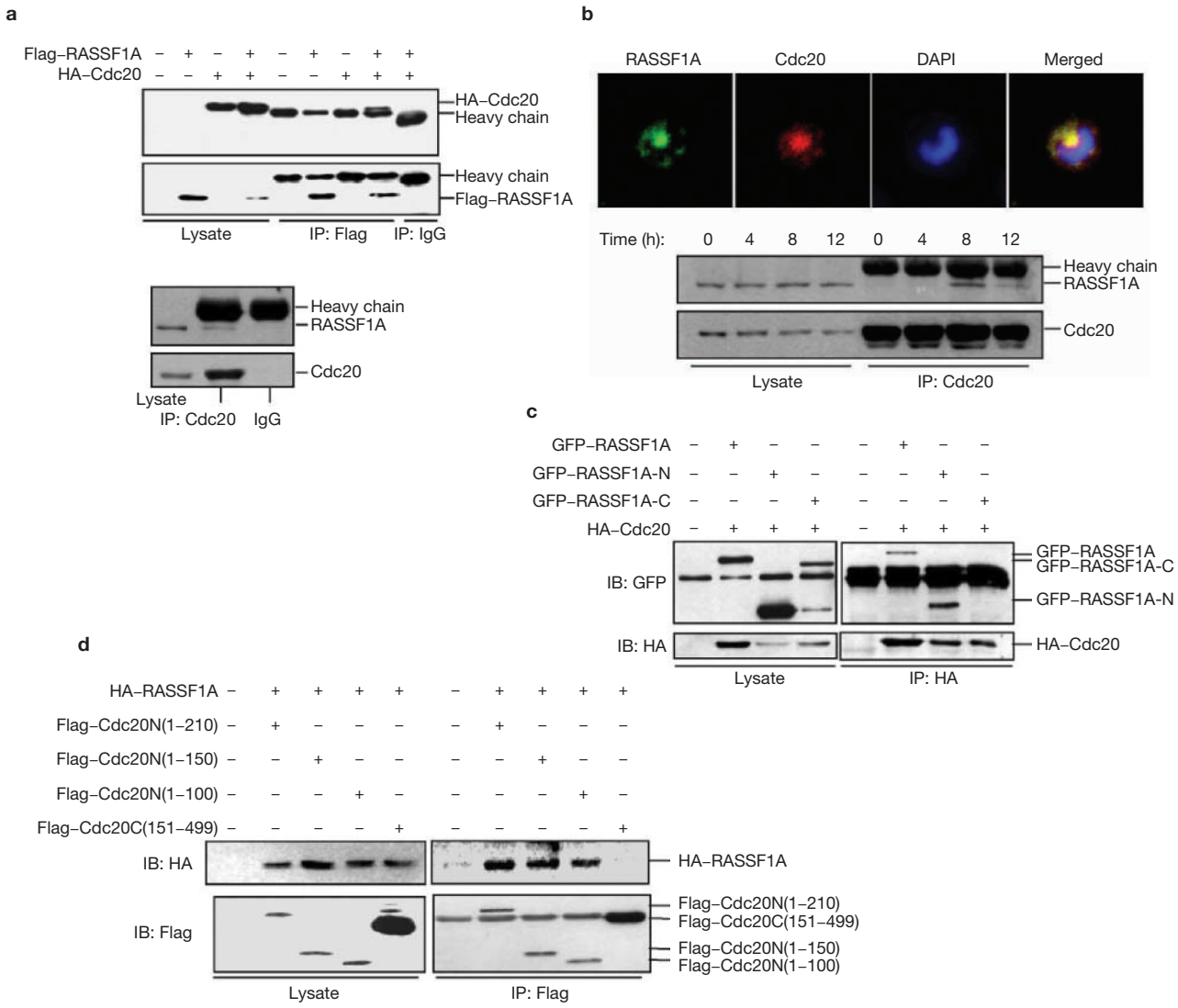

Figure 2 RASSF1A interacts with Cdc20. (**a**) Lysates of 293T cells expressing Flag–RASSF1A or HA–Cdc20, as indicated, were subjected to immunoprecipitation (IP) with anti-Flag or control mouse IgG, and the resulting precipitates (as well as cell lysates) were subjected to immunoblotting with anti-HA or anti-Flag (top). Immunoprecipitates prepared from HeLa cells with anti-Cdc20 or control rabbit IgG were analysed with anti-RASSF1(A4) and anti-Cdc20 (bottom). (**b**) HeLa cells were stained with anti-RASSF1(A4) (green), anti-Cdc20 (red) and DAPI (blue). The merged image shows co-localization of RASSF1A and Cdc20 to spindle fibres and spindle poles at prometaphase (top). Lysates of HeLa cells released from thymidine block for the indicated times were subjected to IP with anti-Cdc20, and the resulting precipitates were analysed with anti-RASSF1(A4) and anti-Cdc20 (bottom). (**c**) Anti-HA IP prepared from 293T cells expressing GFP–RASSF1A mutants or HA–Cdc20, as indicated, were analysed with anti-GFP and anti-HA. IB, immunoblotting. (**d**) Anti-Flag IP prepared from 293T cells expressing Flag–Cdc20 mutants or HA–RASSF1A, as indicated, were analysed with anti-Flag and anti-HA.

We next tested whether a loss of RASSF1A leads to defective regulation of mitotic progression as a result of premature activation of the APC. HeLa cells depleted of RASSF1A by RNAi with the RASSF1A-1 siRNA did not differ from control cells (those transfected with the empty vector or with that for RASSF1A-3 siRNA) in the kinetics of cell cycle progression from S phase to prometaphase (Fig. 5a). However, whereas the control cells had progressed to G1 phase by 16 h after release from thymidine block, RASSF1A-depleted cells had returned to G1 within 14 h, indicating that mitotic progression might have been accelerated by the loss of RASSF1A. Consistently, the destruction of cyclins A and B was initiated earlier in the RASSF1A-deficient cells than in control cells (Fig. 5b), and the level of cyclin B polyubiquitination at prometaphase was markedly greater in the RASSF1A-depleted cells (Fig. 5c). Time-lapse microscopy also revealed that mitotic progression from metaphase to telophase was about 15–20 min faster in the RASSF1A-deficient cells ($n = 8$) than in control cells ($n = 6$) (Fig. 5d). In addition, expression of RASSF1A with a silent mutation within the region targeted by the RASSF1A-1 siRNA was not affected by the RASSF1A-1 siRNA and rendered the cells resistant to the effects of this siRNA on cell cycle progression, indicating a specificity of RNAi (see Supplementary Information, Fig. S1a–c). Restoration of RASSF1A expression in RASSF1A-deficient A549 cells also normalized the accelerated mitotic progression and the premature destruction of cyclins A and B apparent in these cells (see Supplementary Information, Fig. S2).

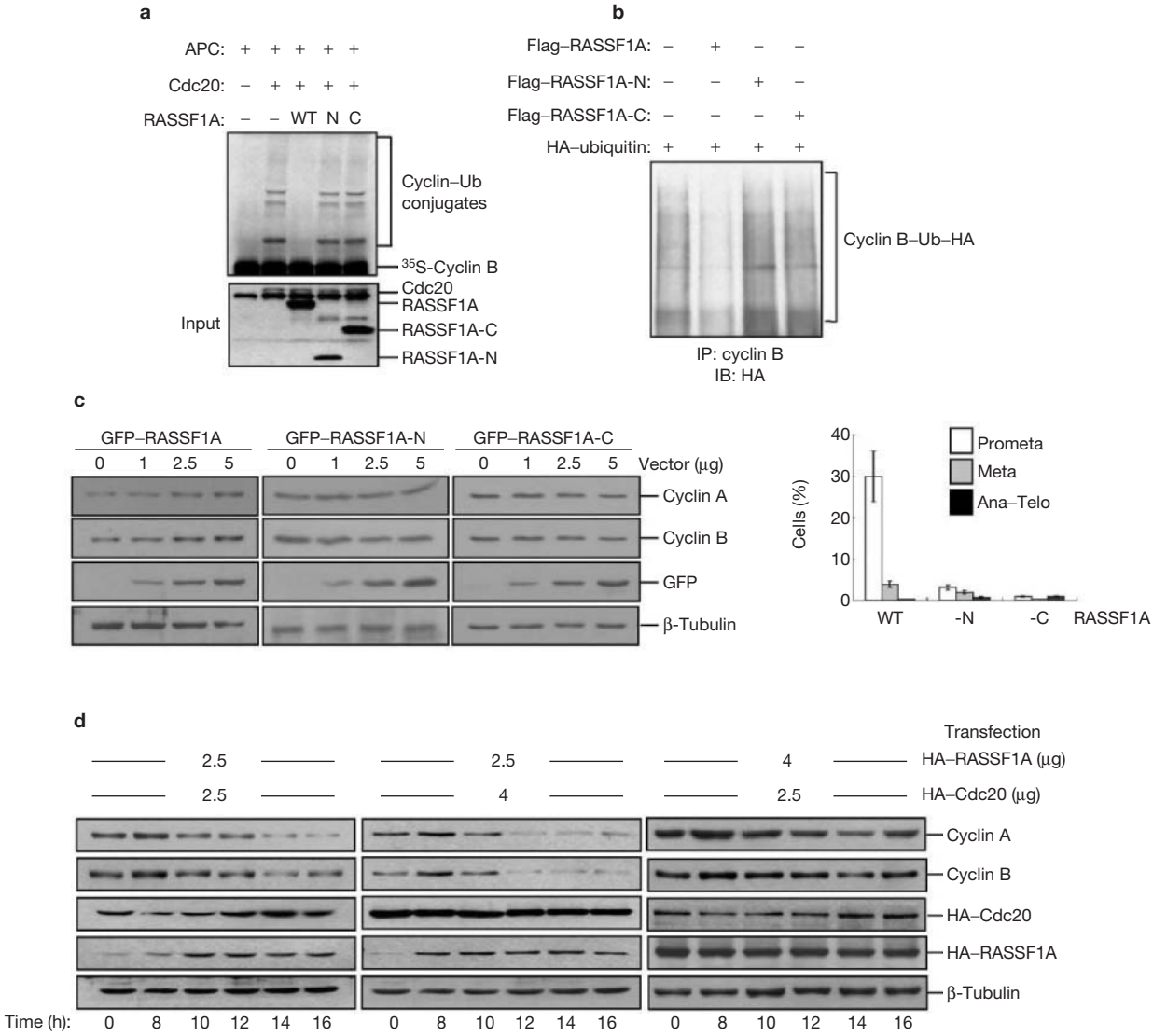

Figure 3 RASSF1A regulates APC–Cdc20 activity. (**a**) The APC was purified from mitotic HeLa cells with anti-Cdc27 and assayed for ubiquitin ligase activity with a ^{35}S-labelled *in vitro*-translated N-terminal fragment of *Xenopus* cyclin B1 (residues 1–102) in the presence of Cdc20 and RASSF1A (wild type, WT), RASSF1A-N or RASSF1A-C (top). The relative amounts of RASSF1A proteins and Cdc20 in the reaction mixtures are also indicated by immunoblotting (bottom). Ub, ubiquitin. (**b**) Lysates of 293T cells co-transfected with vectors for HA–ubiquitin and Flag–RASSF1A mutants, as indicated, were released from thymidine block for 8 h and subjected to immunoprecipitation (IP) with anti-cyclin B, and the resulting precipitates were analysed with anti-HA. IB, immunoblotting. (**c**) Lysates of 293T cells transfected with various amounts of vectors for GFP–RASSF1A mutants, as indicated, were subjected to immunoblotting for the indicated proteins (left). HeLa cells were transfected with vectors for GFP–RASSF1A mutants, as indicated, and the percentages of GFP–positive cells in each mitotic phase were determined; data are means ± s.e.m. from three independent experiments (right). (**d**) 293T cells co-transfected with the indicated amounts of HA–RASSF1A and HA–Cdc20 vectors were released from thymidine block for the indicated times, after which cell lysates were subjected to immunoblotting for the indicated proteins.

Taken together, these results indicate that RASSF1A might control the timing of normal mitotic progression from prometaphase to telophase by regulating APC–Cdc20 activity.

Finally, we examined mitotic events such as centrosome separation, spindle formation and chromosome segregation in normal human foreskin fibroblasts (FSFs) depleted of RASSF1A by infection with a retrovirus-based siRNA vector (Fig. 5e). Almost all control cells in interphase contained one or two centrosomes juxtaposed to the nucleus (Fig. 5f). In contrast, a substantial proportion of RASSF1A-depleted FSFs contained more than two centrosomes (Fig. 5g). In addition, the loss of RASSF1A resulted in various mitotic spindle abnormalities including the formation of multipolar spindles, misalignment of chromosomes, and lagging chromosomes (Fig. 5i–o). These abnormalities were corrected by co-transfection of the cells with a vector for RASSF1A containing a silent mutation rendering it resistant to the RASSF1A-1 siRNA (see Supplementary Information, Fig. S1d, e).

In conclusion, RASSF1A is an efficient negative regulator of APC–Cdc20 during mitotic progression. The activity of APC–Cdc20 must be strictly regulated by negative regulators, including Emi1,

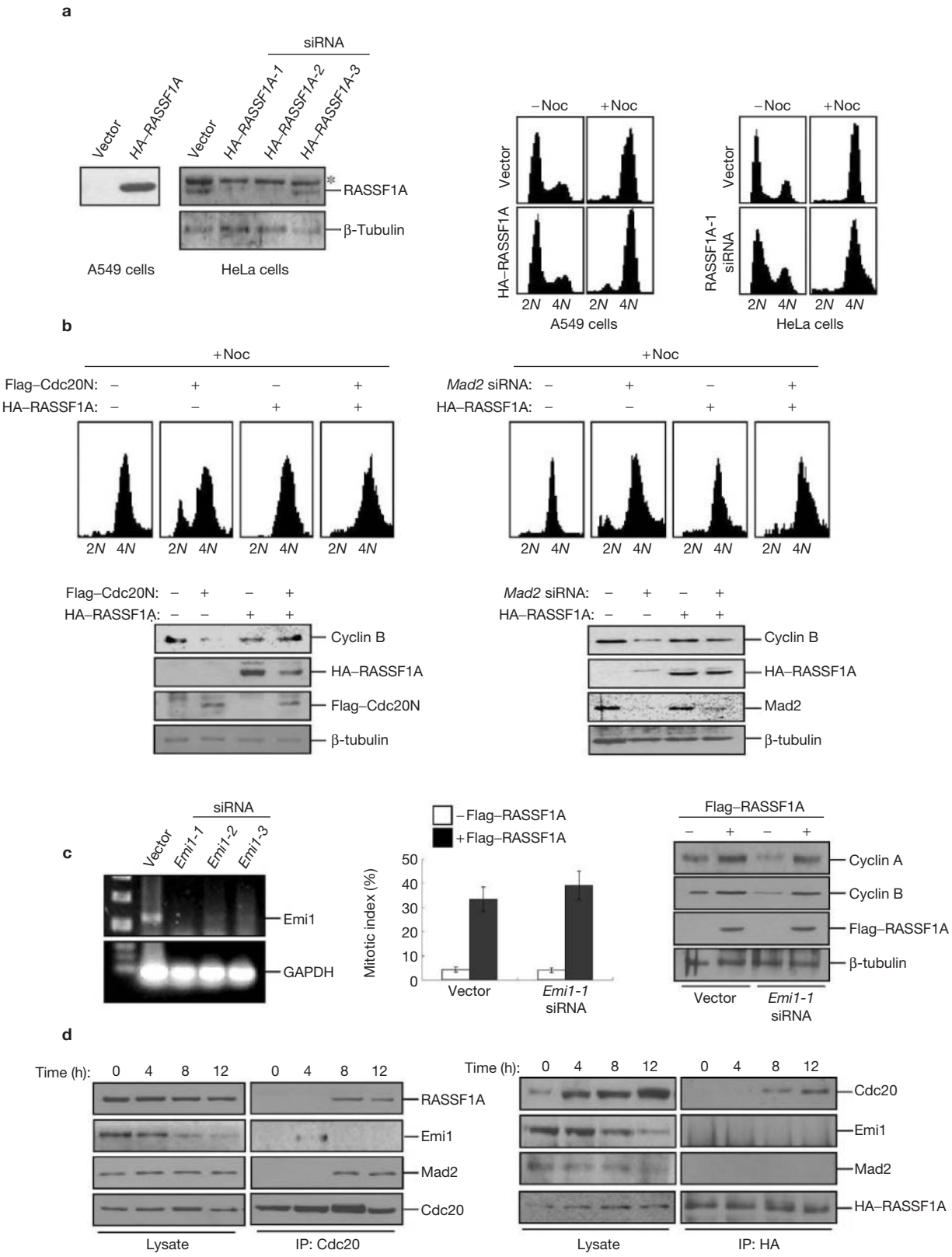

RASSF1A and Mad2, at specific times and at specific subcellular locations during mitotic progression. We have shown that these negative regulators seem to associate differentially with Cdc20 during mitotic progression. The function of RASSF1A seems to be distinct from and independent of that of Emi1, as indicated by our observations that RASSF1A is required for mitotic progression at prometaphase, and associates with Cdc20 after Emi1 is degraded. Unlike Emi1 (ref. 14), RASSF1A does not bind to Cdh1 or inhibit APC-Cdh1 activity *in vitro*

Figure 4 RASSF1A inhibits APC–Cdc20 independently of the spindle assembly checkpoint or Emi1. (**a**) Lysates of A549 cells stably transfected with a retroviral vector for HA–RASSF1A were analysed with anti-HA. Lysates of HeLa cells stably transfected with a vector for RASSF1A-1, -2 or -3 siRNA were analysed with anti-RASSF1(331) and anti-β-tubulin (asterisk indicates a non-specific band). The RASSF1A-3 siRNA failed to downregulate RASSF1A. These cells were also incubated for 20 h in the absence or presence of nocodazole (200 ng ml^{-1}) (NOC) before determination of their DNA content by flow cytometry. (**b**) HeLa cells were co-transfected with vectors for HA–RASSF1A and either a Flag-tagged N-terminal fragment of Cdc20 (Cdc20N, residues 1–101) (left) or a Mad2 siRNA (right). After treatment with nocodazole as described in **a**, the cells were subjected to flow cytometric analysis of DNA content (top) and to immunoblotting for the indicated proteins (bottom). (**c**) RNAs of HeLa cells transfected with a vector for Emi1-1, -2 or -3 siRNA and was subjected to reverse transcriptase polymerase chain reaction with primers specific for Emi1 or glyceraldehyde-3-phosphate dehydrogenase (GAPDH) cDNAs (left). HeLa cells expressing the Emi1-1 siRNA were transiently transfected with a vector for Flag–RASSF1A and stained with anti-Flag and anti-β-tubulin for determination of the mitotic index of Flag-positive cells; data are means ± s.e.m. from three independent experiments (middle). Cell lysates were also subjected to immunoblotting for the indicated proteins (right). (**d**) Lysates of HeLa cells released from thymidine block for the indicated times were subjected to immunoprecipitation (IP) with anti-Cdc20, and the resulting precipitates were analysed with anti-RASSF1(A4), anti-Emi1, anti-Mad2 and anti-Cdc20 (left). A549 cells stably expressing HA–RASSF1A were released from thymidine block for the indicated times and then subjected to IP with anti-HA, and the resulting precipitates were analysed with anti-Cdc20, anti-Emi1, anti-Mad2 and anti-RASSF1(A4) (right).

(data not shown). Overexpression of RASSF1A also induced a more pronounced mitotic block at early prometaphase (39% of cells) than did overexpression of Emi1 (6–10% of cells)[12,14]. Thus, RASSF1A and Emi1 are likely to be required for inhibition of the APC at early prometaphase and at S and G2-prophase, respectively[12–14,17,22]. The function of RASSF1A also seems to be independent of that of Mad2, given that RASSF1A prevents the destruction of cyclin A, which is independent of spindle checkpoint activation or of Mad2 (ref. 13). In addition, RASSF1A-depleted cells show normal spindle checkpoint control. Taking these results together, we therefore propose that RASSF1A acts in early prometaphase, before activation of the spindle checkpoint (late prometaphase) and after Emi1 destruction (prophase), to prevent the degradation of mitotic cyclins and to delay mitotic progression beyond metaphase. Given that the destruction of cyclin B is initiated at the spindle poles and then proceeds sequentially on the spindle and in the cytoplasm[23], RASSF1A might contribute to the inhibition of APC–Cdc20 at centrosomes and on spindle fibres, where we have shown RASSF1A to be localized.

Mutations in various genes that contribute to mitotic regulation, including those for the adenomatous polyposis coli protein, Bub1 and securin, induce chromosomal instability in cancer cells[24–27]. Therefore, a loss of RASSF1A also might contribute to carcinogenesis or tumour progression by inducing both an abnormality in the timing of mitotic progression and chromosome instability. Consistent with this hypothesis was our observation that tumour size was markedly greater in athymic nude mice injected with RASSF1A-deficient HeLa cells than in those injected with control HeLa cells (see Supplementary Information, Fig. S3). The generation of mice with mutations in *RASSF1A* and characterization of their susceptibility to chromosomal instability and cancer should therefore provide insight into this issue. □

METHODS

Plasmid construction. The human complementary DNAs for RASSF1A or RASSF1C were cloned into pSG5 (Stratagene) or pMSCV-Puro (Clontech) for the expression of HA- or Flag-tagged proteins, into pRSET (Invitrogen) or into pEGFP (Clontech). The cDNAs for RASSF1A or human Cdc20 deletion mutants were cloned into pEGFP or pSG5. For generating RASSF1A siRNA vectors, the annealed oligonucleotides containing RASSF1A cDNA sequences (RASSF1A-1, sense 5′- GACCTCTGTGGCGACTTCA-3′; RASSF1A-2, sense 5′-TGTGGAGTGGGAGACACCT-3′; RASSF1A-3, sense 5′- GGCCCTGAGCTTTGTCCTG-3′) were ligated into pSUPER or pSUPER-retro (Oligoengine) that had been digested with *Bgl*II and *Hin*dIII. The vector for Mad2 siRNA was generated by cloning an oligonucleotide containing human Mad2 cDNA sequence (sense 5′-GTGGTGAGGTCCTGGAAAG-3′) into pSUPER. In addition, Emi1 siRNAs were designed on the basis of the human Emi1 cDNA sequence as described[14]. The cDNA for the RASSF1A silent mutant (TGT→TGC in the RASSF1A-1 siRNA target sequence) was generated by site-directed mutagenesis with the use of a QuickChange kit (Stratagene) and was subcloned into either pSG5 or pMSCV-Puro.

Cell culture and transfection. 293T cells, HeLa cells and FSFs were cultured in DMEM medium supplemented with 10% FBS. For thymidine block and release experiments, cells were incubated for 16 h with 2 mM thymidine (Sigma), washed, and then incubated in medium without thymidine. Unless otherwise indicated, 293T cells were transiently transfected with plasmids by $CaCl_2$ precipitation, and HeLa cells were transfected with the use of the Effectene transfection reagent (Qiagen). For stable expression of siRNAs in HeLa cells, the cells were co-transfected with the corresponding pSUPER vector (2 μg) and pcDNA-puro (0.2 μg) and were then selected in the presence of puromycin (3 μg ml^{-1}). Retroviruses were produced by transfection of 293T packaging cells with the corresponding pSUPER-retro vector or pMSCV-Puro vector; after 48 h the virus-containing culture supernatants were used to infect FSFs and the cells were then selected for 5 days in the presence of puromycin (3 μg ml^{-1}), as described previously[28].

Antibodies. Anti-RASSF1(331) antibodies were generated by injecting rabbits with a keyhole-limpet-haemocyanin-conjugated peptide corresponding to the C-terminal 14 amino acids of human RASSF1 (RQKIQEALHACPLG), and anti-RASSF1(A4) antibodies were generated by injecting mice with purified His_6-tagged RASSF1A. Other antibodies included mouse monoclonal antibodies against HA (Roche), against Flag or γ-tubulin (Sigma), against α- or β-tubulin (Oncogene), against phospho-histone H3 (Calbiochem), against cyclin B or Cdc20 (Santa Cruz Biotechnology), against Mad2 (Transduction Laboratories), or against GFP (Zymed) as well as rabbit polyclonal antibodies against HA, β-tubulin, Cdc20 or cyclin A (Santa Cruz Biotechnology) or against Emi1 (Abcam).

Immunofluorescence. Cells were grown on chamber slides (LabTakII; Nunc). After transfection or drug treatment, the cells were washed twice with PBS, fixed in ice-cold methanol, washed with PBS, and then incubated for 30 min with 5% normal goat serum (Sigma) in PBS. They were then exposed consecutively to primary antibodies and to rhodamine-conjugated or fluorescein isothiocyanate (FITC)-conjugated goat antibodies against rabbit or mouse immunoglobulin G (IgG) (Santa Cruz Biotechnology). Slides were mounted in medium containing 4′,6-diamidino-2-phenylindole (DAPI) and imaged with a Zeiss Axiophot microscope, a Nikon inverted microscope equipped with a Hamamatsu Orca CCD camera, or a confocal laser-scanning microscope (CLSM Bio-Rad 1024). Data were processed with Adobe Photoshop 5.5 software.

Cell cycle analysis. Cells were co-transfected with pcDNA-CD4 and HA–RASSF1 vectors at a mass ratio of 1:10, collected at various times after transfection, and incubated for 1 h at 4 °C with FITC-conjugated anti-CD4 (Calbiochem). They were then washed three times with PBS, fixed in 70% ethanol, stained with propidium iodide (25 μg ml^{-1}) (Sigma), and incubated for 30 min at 37 °C with RNase A (20 μg ml^{-1}) (Roche). The DNA content of the cells was then evaluated by flow cytometry with a FACScan instrument (Becton Dickinson). Linear red fluorescence (FL2) in green CD4-expressing cells was analysed.

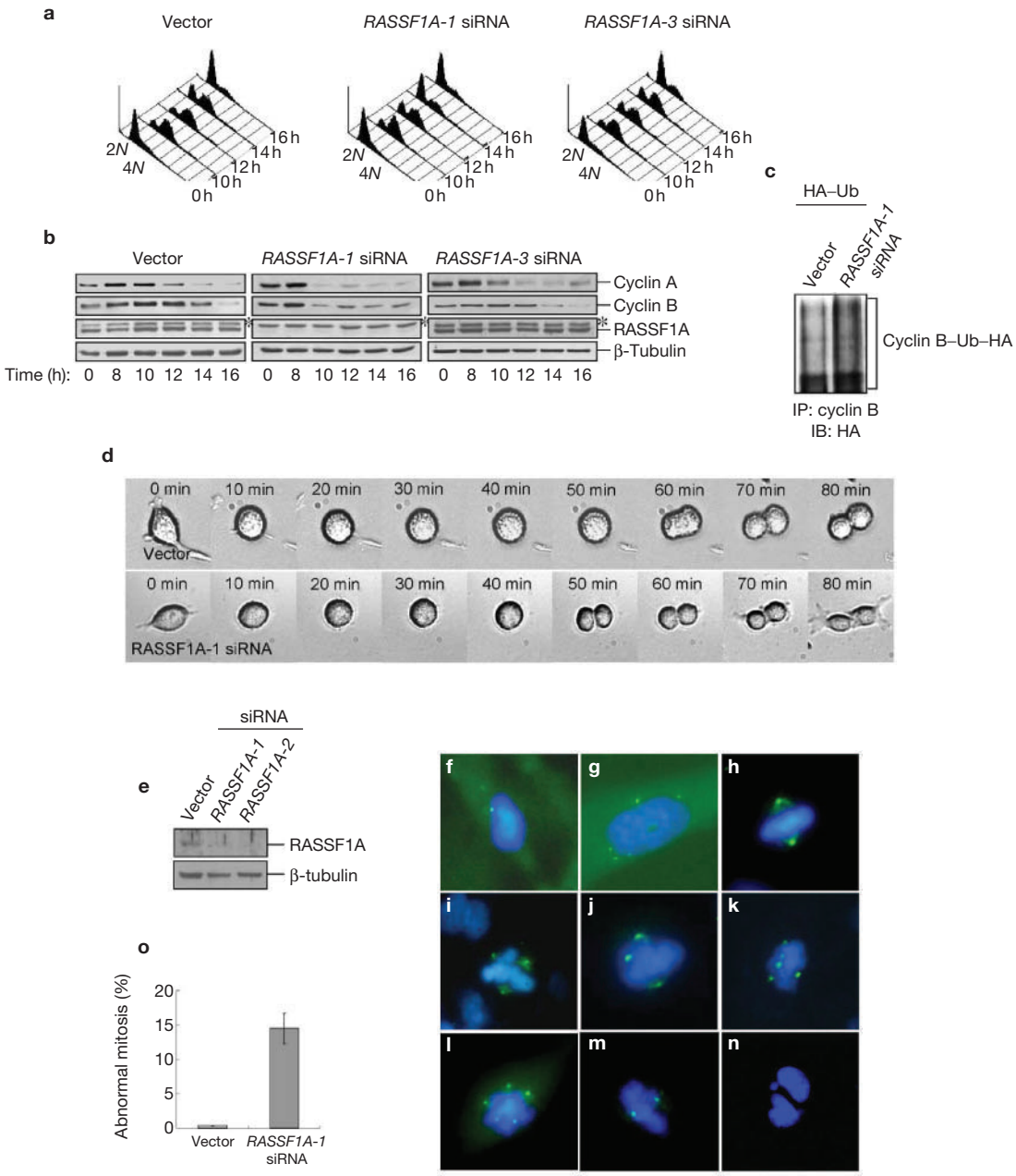

Figure 5 Loss of RASSF1A results in acceleration of mitotic progression and in mitotic abnormalities. (**a**) HeLa cells transfected with RASSF1A-1 or -3 siRNA were released from thymidine block for the indicated times before analysis of DNA content by flow cytometry. (**b**) Cells treated as in **a** were subjected to immunoblotting for the indicated proteins. The asterisk indicates a non-specific band. (**c**) HeLa cells co-transfected with vectors for RASSF1A-1 siRNA and HA–ubiquitin (HA–Ub) were released from thymidine block for 8 h and subjected to immunoprecipitation (IP) with anti-cyclin B, and the resulting precipitates were analysed with anti-HA. IB, immunoblotting. (**d**) HeLa cells transfected with RASSF1A-1 siRNA were imaged by time-lapse microscopy during mitotic progression from late prophase (time 0). (**e**) Lysates of FSFs transfected with a retroviral vector for RASSF1A-1 siRNA were analysed with anti-RASSF1(A4) and anti-β-tubulin. (**f**–**n**) Centrosome abnormalities, multipolar spindles, and misaligned or lagging chromosomes in FSFs depleted of RASSF1A. FSFs transfected with RASSF1A-1 siRNA (**g**, **i**–**n**) or the empty vector (**f**, **h**) were stained with anti-γ-tubulin (green) and DAPI (blue). **f**, **h**, Normal interphasic and mitotic FSFs, respectively. **g**, Interphasic RASSF1A-depleted FSFs with multiple centrosomes. **i**–**l**, Mitotic RASSF1A-depleted FSFs with centrosome abnormalities, multipolar spindles and misaligned chromosomes. **m**, **n**, RASSF1A-depleted FSFs with lagging chromosomes. **o**, RASSF1A-depleted FSFs were scored for abnormal mitosis. Data are means ± s.e.m. from three independent experiments.

Immunoprecipitation. Cells were released from thymidine block and lysed in a lysis buffer containing 50 mM Tris-HCl (pH 7.5), 150 mM NaCl, 1 mM EDTA, 1 mM $MgCl_2$ and 0.5% Triton X-100. Lysates were cleared by centrifugation at 15,000*g* for 20 min at 4 °C and analysed by SDS–PAGE. For immunoprecipitation, lysates were incubated with antibodies coupled to protein G–agarose (Oncogene) for 1 h at 4 °C. The immunoprecipitates were washed four times with lysis buffer and then subjected to immunoblotting.

Time-lapse microscopy. Cells were placed in a microincubation chamber (Olympus IX-IBC) on the stage of an Olympus IX-71 microscope, which was heated to 37 °C and equipped with a CO_2 supply as well as with a charge-coupled device (CCD) camera (Olympus CoolSNAP cf color 10L) mounted at the side port. The cooled CCD camera was controlled by PVCAM 2.6.3 software (Olympus). Time-lapse series were generated by collecting photographs every 5-min; the photos were then converted to 8-bit images and processed by Adobe Photoshop 5.5 software.

***In vitro* assay of APC activity.** The APC was purified from extracts of mitotic HeLa cells by immunoprecipitation with anti-cdc27 beads (Santa Cruz Biotechnology). *In vitro* assays of the ubiquitination of an N-terminal fragment of *Xenopus* cyclin B were performed as described[29]. In brief, the purified APC was incubated for 1 h at 4 °C with *in vitro*-translated Cdc20 (5 μl) that had been preincubated for 30 min at 4 °C in the presence of *in vitro*-translated full-length RASSF1A, RASSF1A-N or RASSF1A-C (10 μl). After being washed twice, the immunoprecipitates were then supplied with purified UbcH10 (Boston Biochem), E1 (Boston Biochem), an ATP-regenerating system (7.5 mM creatine phosphate, 1 mM ATP, 1 mM $MgCl_2$, 0.1 mM EGTA, rabbit creatine phosphokinase type I (30 U ml^{-1}) (Sigma)), ubiquitin (1.25 mg ml^{-1}) (Sigma) and a ^{35}S-labelled *in vitro*-translated fragment of cyclin B. The reactions were stopped after 60 min at 25 °C and the extent of substrate ubiquitination was then analysed by SDS–PAGE and autoradiography.

***In vivo* ubiquitination assays.** Cells transfected with a plasmid encoding HA-tagged human ubiquitin were subjected to thymidine block and release and then analysed for ubiquitination *in vivo* as described[30]. They were lysed by incubation for 10 min at 95 °C with 2 volumes of TBS (10 mM Tris-HCl (pH 7.5), 150 mM NaCl) containing 2% SDS. After the addition of 8 volumes of 1% Triton X-100 in TBS, the lysates were sonicated for 2 min and then incubated with protein G–agarose. The beads were removed by centrifugation, and the lysates were then subjected to immunoprecipitation with anti-cyclin B coupled to protein G–agarose. The beads were washed first with 0.5 M LiCl in TBS and then twice with TBS, boiled, and subjected to immunoblot analysis with anti-HA.

Note: Supplementary Information is available on the Nature Cell Biology website.

ACKNOWLEDGEMENTS

We thank M. White and C. H. Lee for RASSF1A and Cdc20 cDNAs, respectively, and B. S. Suh for comments on the manuscript. This work was supported by grants from the 21st Century Frontier Functional Human Genome Project of KISTEP (Ministry of Science and Technology of Korea) and the Biomedical Research Program of KISTEP to D.-S.L., by a grant from the National Creative Research Program of KISTEP to E.-J.C, and by a grant from the Korea Health 21 R&D Project (02-PJ-PG10-20802-0012) to H.K. D.-S.L. was also supported by a grant from the Korea National Cancer Center Control Program (0320370-1).

COMPETING FINANCIAL INTERESTS

The authors declare that they have no competing financial interests.

Received 23 August 2003; accepted 5 January 2003
Published online at http://www.nature.com/naturecellbiology.

1. Dammann, R. *et al.* Epigenetic inactivation of a RAS association domain family protein from the lung tumour suppressor locus 3p21.3. *Nature Genet.* **25,** 315–319 (2000).
2. Astuti, D. *et al.* RASSF1A promoter region CpG island hypermethylation in phaeochromocytomas and neuroblastoma tumours. *Oncogene* **20,** 7573–7577 (2001).
3. Burbee, D. G. *et al.* Epigenetic inactivation of RASSF1A in lung and breast cancers and malignant phenotype suppression. *J. Natl. Cancer Inst.* **93,** 691–699 (2001).
4. Dammann, R., Takahashi, T. & Pfeifer, G. P. The CpG island of the novel tumor suppressor gene RASSF1A is intensely methylated in primary small cell lung carcinomas. *Oncogene* **20,** 3563–3567 (2001).
5. Dreijerink, K. *et al.* The candidate tumor suppressor gene, RASSF1A, from human chromosome 3p21.3 is involved in kidney tumorigenesis. *Proc. Natl Acad. Sci. USA* **98,** 7504–7509 (2001).
6. Lo, K. W. *et al.* High frequency of promoter hypermethylation of RASSF1A in nasopharyngeal carcinoma. *Cancer Res.* **61,** 3877–3881 (2001).
7. King, R. W., Deshaies, R. J., Peters, J. M. & Kirschner, M. W. How proteolysis drives the cell cycle. *Science* **274,** 1652–1659 (1996).
8. Zachariae, W. & Nasmyth, K. Whose end is destruction: cell division and the anaphase-promoting complex. *Genes Dev.* **13,** 2039–2058 (1999).
9. Jallepalli, P. V. & Lengauer, C. Chromosome segregation and cancer: cutting through the mystery. *Nature Rev. Cancer* **1,** 109–117 (2001).
10. Peters, J. M. The anaphase-promoting complex: proteolysis in mitosis and beyond. *Mol. Cell* **9,** 931–943 (2002).
11. Visintin, R., Prinz, S. & Amon, A. CDC20 and CDH1: a family of substrate-specific activators of APC-dependent proteolysis. *Science* **278,** 460–463 (1997).
12. Reimann, J. D., Gardner, B. E., Margottin-Goguet, F. & Jackson, P. K. Emi1 regulates the anaphase-promoting complex by a different mechanism than Mad2 proteins. *Genes Dev.* **15,** 3278–3285 (2001).
13. Reimann, J. D. *et al.* Emi1 is a mitotic regulator that interacts with Cdc20 and inhibits the anaphase promoting complex. *Cell* **105,** 645–655 (2001).
14. Hsu, J. Y., Reimann, J. D., Sorensen, C. S., Lukas, J. & Jackson, P. K. E2F-dependent accumulation of hEmi1 regulates S phase entry by inhibiting APC(Cdh1). *Nature Cell Biol.* **4,** 358–366 (2002).
15. Vos, M. D., Ellis, C. A., Bell, A., Birrer, M. J. & Clark, G. J. Ras uses the novel tumor suppressor RASSF1 as an effector to mediate apoptosis. *J. Biol. Chem.* **275,** 35669–35672 (2000).
16. Shivakumar, L., Minna, J., Sakamaki, T., Pestell, R. & White, M. A. The RASSF1A tumor suppressor blocks cell cycle progression and inhibits cyclin D1 accumulation. *Mol. Cell. Biol.* **22,** 4309–4318 (2002).
17. Margottin-Goguet, F. *et al.* Prophase destruction of Emi1 by the SCF(betaTrCP/Slimb) ubiquitin ligase activates the anaphase promoting complex to allow progression beyond prometaphase. *Dev. Cell* **4,** 813–826 (2003).
18. Zhang, Y. & Lees, E. Identification of an overlapping binding domain on Cdc20 for Mad2 and anaphase-promoting complex: model for spindle checkpoint regulation. *Mol. Cell. Biol.* **21,** 5190–5199 (2001).
19. Brummelkamp, T. R., Bernards, R. & Agami, R. A system for stable expression of short interfering RNAs in mammalian cells. *Science* **296,** 550–553 (2002).
20. Luo, X., Tang, Z., Rizo, J. & Yu, H. The Mad2 spindle checkpoint protein undergoes similar major conformational changes upon binding to either Mad1 or Cdc20. *Mol. Cell* **9,** 59–71 (2002).
21. Martin-Lluesma, S., Stucke, V. M. & Nigg, E. A. Role of Hec1 in spindle checkpoint signaling and kinetochore recruitment of Mad1/Mad2. *Science* **297,** 2267–2270 (2002).
22. Guardavaccaro, D. *et al.* Control of meiotic and mitotic progression by the F box protein β-Trcp1 in vivo. *Dev. Cell* **4,** 799–812 (2003).
23. Raff, J. W., Jeffers, K. & Huang, J. Y. The roles of Fzy/Cdc20 and Fzr/Cdh1 in regulating the destruction of cyclin B in space and time. *J. Cell Biol.* **157,** 1139–1149 (2002).
24. Cahill, D. P. *et al.* Mutations of mitotic checkpoint genes in human cancers. *Nature* **392,** 300–303 (1998).
25. Fodde, R. *et al.* Mutations in the APC tumour suppressor gene cause chromosomal instability. *Nature Cell Biol.* **3,** 433–438 (2001).
26. Kaplan, K. B. *et al.* A role for the Adenomatous Polyposis Coli protein in chromosome segregation. *Nature Cell Biol.* **3,** 429–432 (2001).
27. Jallepalli, P. V. *et al.* Securin is required for chromosomal stability in human cells. *Cell* **105,** 445–457 (2001).
28. Lim, D. S. *et al.* ATM phosphorylates p95/nbs1 in an S-phase checkpoint pathway. *Nature* **404,** 613–617 (2000).
29. Fang, G., Yu, H. & Kirschner, M. W. The checkpoint protein MAD2 and the mitotic regulator CDC20 form a ternary complex with the anaphase-promoting complex to control anaphase initiation. *Genes Dev.* **12,** 1871–1883 (1998).
30. Buschmann, T., Fuchs, S. Y., Lee, C. G., Pan, Z. Q. & Ronai, Z. SUMO-1 modification of Mdm2 prevents its self-ubiquitination and increases Mdm2 ability to ubiquitinate p53. *Cell* **101,** 753–762 (2000).

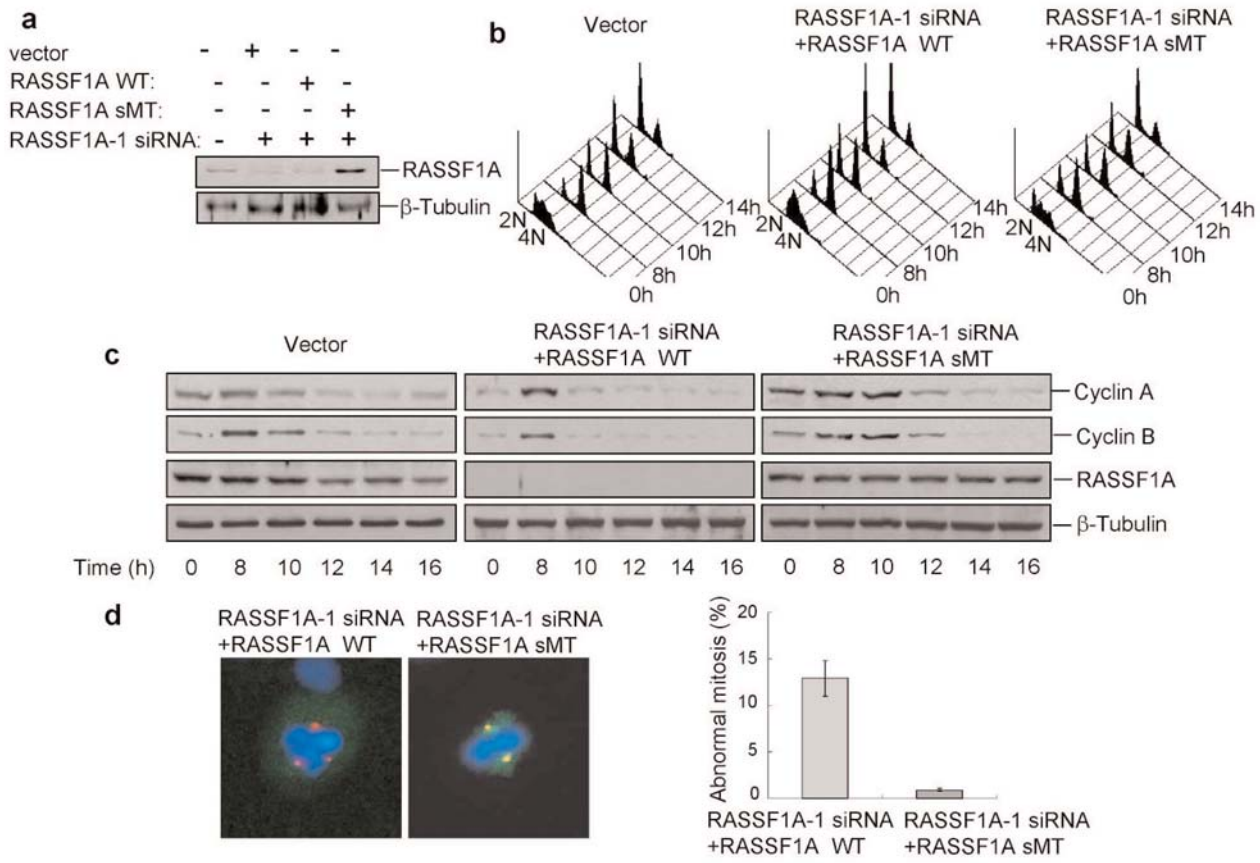

Figure S1 Rescue of the phenotype of RASSF1A-depleted cells by cotransfection of nondegradable RASSF1A construct. **a**, HeLa cells were cotransfected with vectors for RASSF1A-1 siRNA and pcDNA3-RASSF1A wild type (WT) or -RASSF1A mutant (sMT) with one silent third-codon point mutation within the targeted region (GACCTCTG**C**GGCGACTTCA). Cell lysates were subjected to immunoblotting with anti-RASSF1A (A4) and anti–β-tubulin. **b**, Cells treated as in **a** were released from thymidine block for the indicated times before analysis of DNA content by flow cytometry. **c**, Cells treated as in **b** were subjected to immunoblotting for the indicated proteins. **d**, FSFs were cotransfected with retroviral vectors for RASSF1A-1 siRNA and pcDNA3-RASSF1A wild type (WT) or -RASSF1A mutant (sMT) and stained with anti-RASSF1(331) (green), anti–γ-tubulin (red) and DAPI (blue). FSFs coexpressing RASSF1A siRNA and nondegradable RASSF1A were scored for abnormal mitosis. Data are means ± SEM of values from three independent experiments.

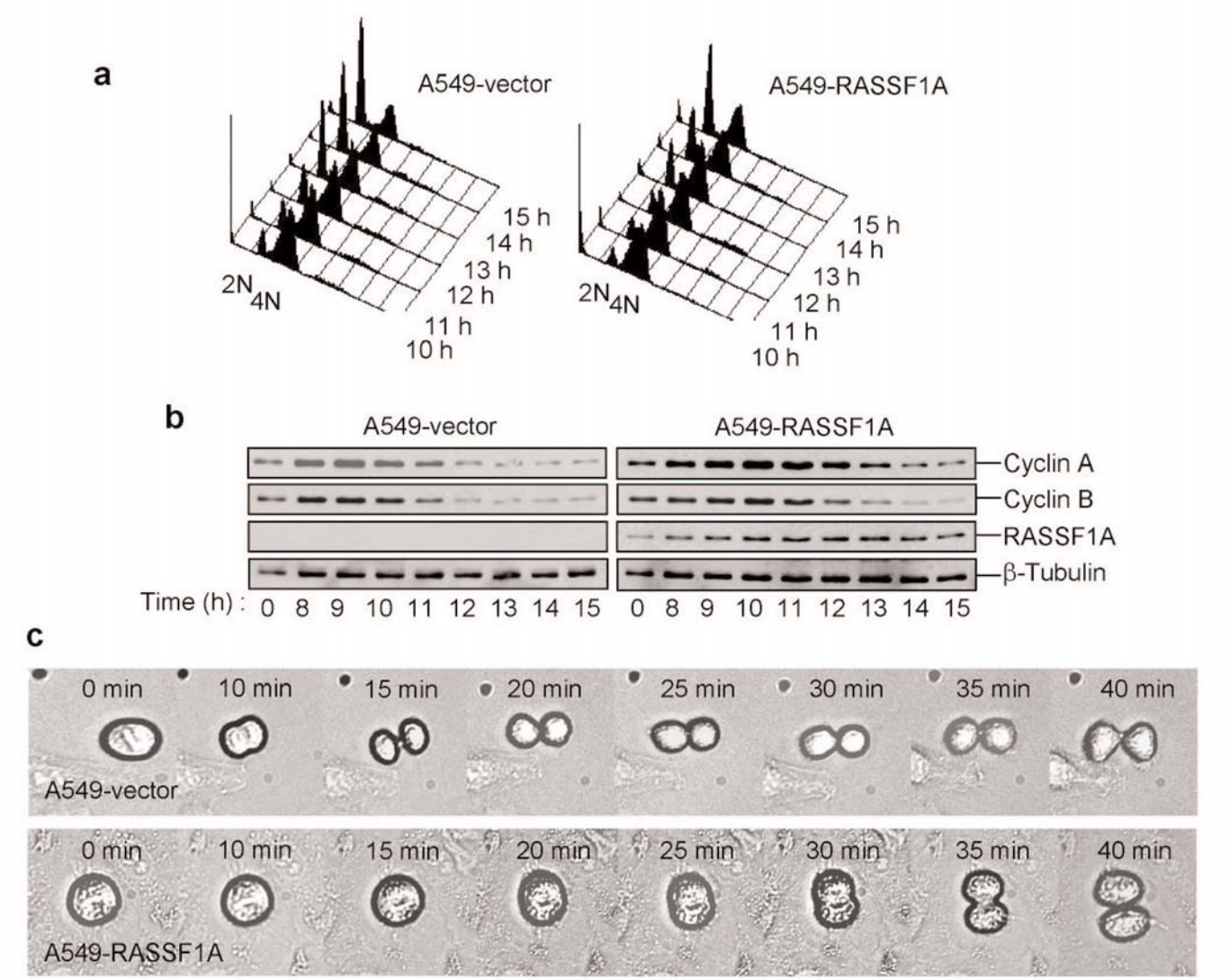

Figure S2 Restoration of RASSF1A expression in A549 cells delays mitotic exit. **a**, A549 cells stably transfected with a retroviral vector for HA-RASSF1A or the corresponding empty vector were released from thymidine block for the indicated times before analysis of DNA content by flow cytometry. **b**, Cells treated as in **a** were subjected to immunoblotting for the indicated proteins. **c**, A549 cells stably transfected with HA-RASSF1A were imaged by time-lapse microscopy during mitotic progression from metaphase (time 0).

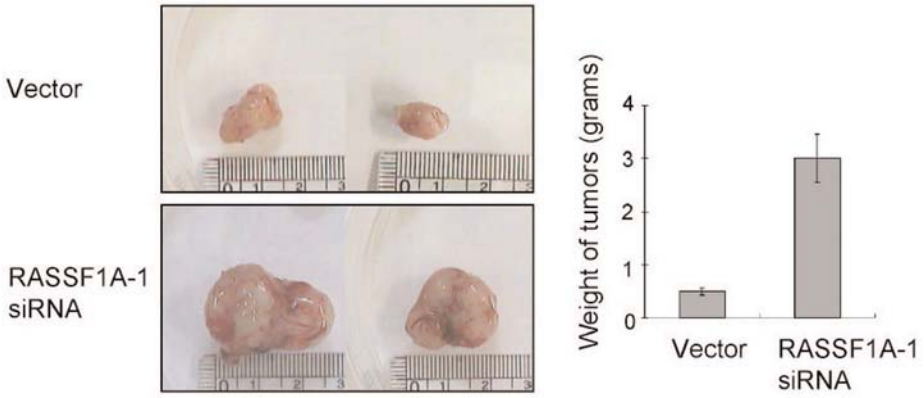

Figure S3 Tumor growth of wild-type and RASSF1A-deficient HeLa cells in athymic nude mice. **a**, Cultures of subconfluent wild-type and RASSF1A-deficient HeLa cells were trypsinized and centrifuged for 5 min. Then, cells were resuspended in serum-free DME and subcutaneously injected into 6-week-old athymic nude mice (BALB/c nu/nu; Charles River Laboratories, Japan). A total volume of 0.1 ml containing 1?10^6 cells was injected into six mice. The mice were euthanized at 28 days postinjection, and the tumors removed from the nude mice are illustrated. **b**, Influence of RASSF1A on the tumors weight. The tumor weight was measured and is presented graphically (mean ± S.D.; n = 6).